

A comparative study on the hydrolysis of acetic anhydride and N,N-dimethylformamide: Kinetic isotope effect, transition-state structure, polarity, and solvent effect

William C. Cooper¹  | Abhinay Chilukoorie¹ | Suhesh Polam¹ | Dane Scott³ | Floyd Wiseman²

¹Department of Physical Sciences, Eastern New Mexico University, Portales, NM, USA

²Department of Chemistry, Davis and Elkins College, Elkins, WV, USA

³Department of Chemistry, East Tennessee State University, Johnson City, TN, USA

Correspondence

William C. Cooper, Department of Physical Sciences, Eastern New Mexico University, 1500 S. Ave. K, Portales, NM 88130, USA.
Email: william.cooper@enmu.edu

Abstract

Recent studies have shown that general-base assisted catalysis is a viable mechanistic pathway for hydrolysis of smaller anhydrides. Therefore, it is the central purpose of the present work to compare and contrast the number of hydrogen atoms in-flight and stationary in the transition state structure of the base-catalyzed mechanisms of 2 hydrolytic reactions as well as determine if any solvent effects occur on the mechanisms. The present research focuses on the hydrolytic mechanisms of N,N-dimethylformamide (DMF) and acetic anhydride in alkali media of varying deuterium oxide mole fractions. Acetic anhydride has been included in this study to enable comparisons with DMF hydrolysis. Comparative studies may give synergistic insight into the detailed structural features of the activated complexes for both systems. Hydrolysis reactions in varying deuterium oxide mole fractions were conducted in concentrations of 2.0M, 2.5M, and 3.0M for DMF and 0.10M for acetic anhydride at 25°C. Studies in varying deuterium mole fractions allow for proton inventory analysis, which sheds light on the number and types of hydrogen atoms involved in the activated complex. For these systems, this type of study can distinguish between direct nucleophilic attack of the hydroxide ion on the carbonyl center and general-base catalysis by the hydroxide ion to facilitate a water molecule attacking the carbonyl center. The numerical data are used to discuss 3 possible mechanisms in the hydrolysis of DMF.

KEYWORDS

Gross-Butler plot, hydroxide-catalyzed acetic anhydride hydrolysis, hydroxide-catalyzed N,N-dimethylformamide hydrolysis, inverse isotope effect, proton inventory studies

1 | INTRODUCTION

Over the years, mechanisms involved in hydrolysis of anhydrides and esters have been extensively studied using titration,^[1,2] calorimetric,^[3–6] conductimetric,^[7,8] spectroscopic,^[9,10] temperature scanning,^[11] combination,^[12,13] pH,^[14] and chromatographic^[15–19] techniques. By studying the mechanism for hydrolysis of N,N-dimethylformamide (DMF), one may infer mechanistic characteristics that occur in other compounds that contain amide structural features,

for example, proteins. One pathway for the breakdown of proteins is through base hydrolysis of the amide backbone structural units. Simpler molecules, such as DMF, are expected to occur by a similar mechanism.^[20–22] Furthermore, studies have been extended to incorporate hydrolysis of sulfanilamides. The reason being is that sulfanilamides contain a functional group sulfonic amide moiety that is contained in compounds of 1 class of antibiotics. The hydrolytic cleavage of a sulfonic amide group should be comparable to a carbonyl amide. The sulfonic amide is formed by a sulfur atom replacing

a carbon atom and an additional =O group has been added to this sulfinyl group. Therefore, obtaining information pertaining to hydrolysis of the sulfonic amide functional moiety of sulfanilamides can provide insight to the metabolic fate of 1 class of antibiotics.^[22–26]

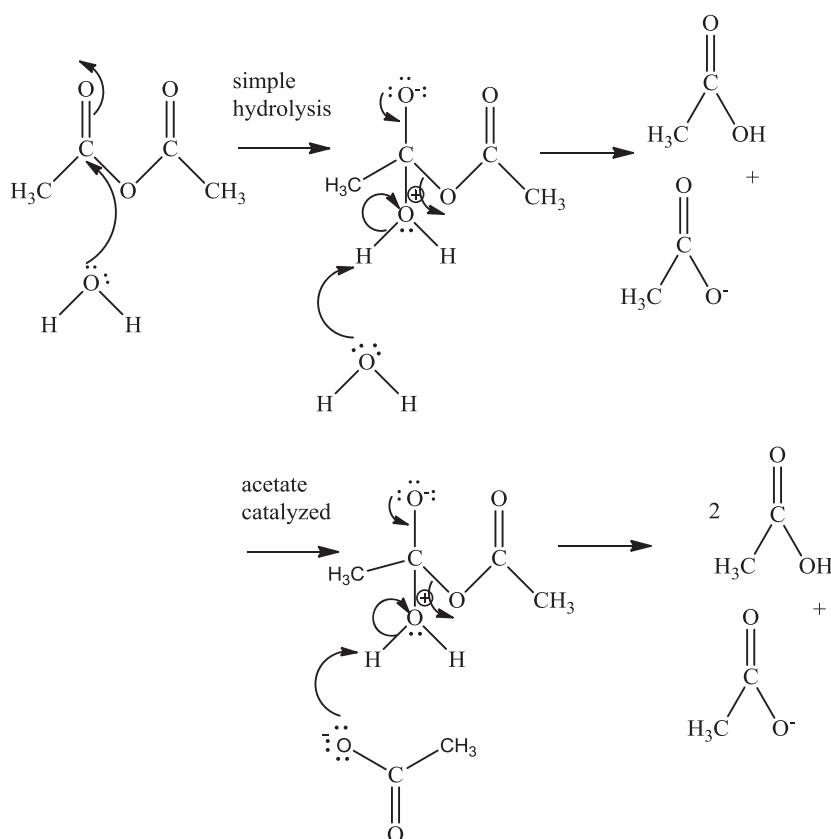
Slebocka-Tilk and coworkers used nuclear magnetic resonance to study the rates of hydroxide-catalyzed hydrolysis on formamide in aqueous media.^[27] These studies aided in determining whether the mechanism involved nucleophilic attack by hydroxide or hydroxide acted as a general base to deprotonate the attacking water molecule. It was determined that both mechanisms could be applied to formamide hydrolysis. However, proton inventory analysis and an inverse isotope effect ($k_{\text{OH}}/k_{\text{OD}} = 0.77 \pm 0.02$) showed that the likely mechanism involves an hydroxide ion solvated by 2 water molecules with 3 water molecules assisting formation of the amide hydrate oxy anion. Marlier and co-workers^[28] used ^{18}O -labeled experiments and concluded that hydroxide acts as a general base to remove a proton from solvating water molecules during the formation of the transition state. From the results of kinetic isotope effect studies of enzyme systems, Xiong and Zhan^[29] and Lynn and Yankwich^[30] have suggested a temperature-dependent interconversion of 2 or more types of active sites (directly or indirectly) through enzyme conformational changes). Mujika et al^[31] suggested that the twist of the amide bond induces an increase on the reaction rate of acid hydrolysis. Linda^[32] and coworkers

mentioned that the rate constants of formation of the tetrahedral intermediate are strongly increased by releasing steric hindrance in the acyl portion as shown by the higher reactivity of *N*-formyl derivatives in comparison with *N*-acetyl and *N*-benzoyl derivatives.

On the other hand, simple- and acetate-catalyzed hydrolysis of acetic anhydride does not show any kind of inverse isotope effect. Wiseman^[14] suggested the transition state structure in simple acetic anhydride hydrolysis probably has 4 protons, whereas acetate catalyzed hydrolysis has 2, as shown in Scheme 1. In Scheme 1 (as well as all of the other schemes), the curved arrows represent movement of electrons.

Proton inventory techniques play a crucial role in elucidating mechanisms by identifying the number and types of hydrogens involved in the transition-state structures. Proton inventory studies, which have been well discussed by Mata-Segreda,^[33] indicate that esters undergo hydrolysis through parallel water catalysis and specific hydrogen ion catalysis.

As it became apparent that there is a significant difference in the deuterium kinetic isotope effect (dkie) between acetic anhydride and DMF, extensive research has been undertaken to understand this difference. Using the procedure described by Laidler and co-worker,^[34] Eyring and Arrhenius graphs were generated to evaluate the activation parameters for these reactions. These graphs shed light on the reasons behind different deuterium kinetic isotope effect (dkie) values between these 2 compounds. For instance, differences in the activation



SCHEME 1 General mechanism: simple- and acetate-catalyzed hydrolysis of acetic anhydride

energy would be identified with large differences in the slopes of the Arrhenius plots. Bunton and coworkers^[35] showed that increasing solvent polarity by increasing the ionic strength decreased the rate constant of the reaction; implying that the transition state is less polar than the reactants. The magnitude of the decrease increases with increasing size of cation or anion. The trend is consistent with work in this paper on sodium chloride effect. They also showed that anions of weak acids, such as formate and nitrite, increase the rate by behaving as general-base catalysts.

This work is aimed at elucidating the number of hydrogens involved in the transition state and mechanism in the hydrolysis of acetic anhydride and DMF. Additionally, this study also shows an inverse kinetic isotope effect ($k_{\text{OH}}/k_{\text{OD}} = 0.51 \pm 0.03$ at 25°C and an hydroxide concentration of 2.0M) for the hydroxide reaction with DMF. This value is consistent with what is observed for other simple amides.^[27,28]

2 | MATERIALS AND INSTRUMENTATION

Deuterium oxide (99.8 %) for the experiments was purchased from Acros and sodium deuterioxide from Cambridge Isotope Laboratories Inc. Water was distilled. Other chemicals such as sodium hydroxide, octanol, cyclohexanol, sodium chloride, and sodium acetate were used as received from VWR. All experiments were performed using a Perkin Elmer Lambda 35 UV/VIS Spectrophotometer.

3 | EXPERIMENTAL

The rate of hydrolysis of acetic anhydride and DMF was determined by monitoring the loss of absorbance at 250 and 230 nm, respectively. For acetic anhydride and water, temperature studies were undertaken to calculate activation energy, enthalpy, and entropy. The rates of hydrolysis of acetic anhydride at 25°C at varying ionic strengths were determined. The kinetic isotope effect in basic conditions was investigated by varying the mole fraction of deuterium oxide in water between 0 and 1 at 7 different temperatures using a precision digital controlled-temperature circulating water bath. For base hydrolysis of acetic anhydride, the sodium hydroxide concentration was 0.12M. In the case of base hydrolysis of DMF, 2.0M, 2.5M, and 3.0M sodium hydroxide/sodium deuterioxide concentrations were used. For example, for acetic anhydride, a 0.503 mole fraction of deuterium content, $\chi_{\text{d}} = 0.503$, was made by adding 1494 μL ($=0.08247$ mol) of D_2O to 1468 μL ($=0.08147$ mol) of H_2O . The density of 1.00 and 1.107 g/mL and a molar mass of 18.01 and 20.02 g/mol were used for H_2O and D_2O , respectively. However, NaOD contributed to the deuterium content as well. In the assay, 0.123M OH^- was obtained by adding 15.0 μL ($=7.426 \text{ e-}7$ mol) of OH^- and

15.0 μL ($=1.098 \text{ e-}6$ mol) OD^- . The NaOD stock concentration was 40 % by weight in D_2O having a density of 1.516 g/mL. A stock concentration of 10.0N was used for NaOH as well that had a density of 1.11 g/mL. Therefore, mole fraction of deuterium $= 0.08247 \text{ mol} + 1.098 \text{ e-}6 \text{ mol} / 0.08147 \text{ mol} + 1.098 \text{ e-}6 \text{ mol} + 7.426 \text{ e-}7 \text{ mol} + 0.08247 \text{ mol}$. If χ_{d} was 0.503, the χ_{h} was $1 - 0.503 = 0.497$. Seven μL of pure acetic anhydride was added to initiate the assay. The total volume in the cuvette was 3 mL. Similarly, 10 μL of pure DMF was added to initiate the assay. A typical assay consisted of collecting abs vs time for 1500 seconds for periods of every second on a Perkin Elmer lambda 35 UV-visible Spectrophotometer. Absorbance was converted to concentration by dividing by the absorptivity. Plots of $-\ln(\text{Conc.})$ versus time yielded a slope from which rate constants were obtained. Solvent polarity effects for acetic anhydride and DMF hydrolyses were studied by conducting the reactions in aqueous solutions of varying mole fractions of cyclohexanol and 1-octanol, and varying sodium chloride concentration.

4 | RESULTS

4.1 | Activation energy (E_{a})

Activation parameters such as activation energy, enthalpy, entropy, and Gibbs free energy were calculated by studying the rate of hydrolysis of acetic anhydride and DMF at varying temperatures. The following analysis is taken from Carroll.^[36] The natural logarithmic form of the Arrhenius equation is

$$\ln k = -\frac{E_{\text{a}}}{RT} + \ln A \quad (1)$$

in which k is the rate constant, E_{a} is the activation energy, A is the pre-exponential factor, R is the gas constant, and T is temperature.

4.2 | Enthalpy, entropy, and Gibbs free energy

According to transition state theory, the rate constant k_{r} is defined by Equation 2 given by Wiseman et al in which the equation is a derivative for the Eyring equation that corrects for nonlinearity.^[37] $\ln(k/T)$ vs $1/T$ were plotted and fitted according to Equation 2 using Logger Pro. The slight departure from linearity in the Arrhenius plots may be attributed to nonlinearity of the heat capacities of activation at lower temperatures or due to the error in measuring the rate constants at lower temperatures.

$$R \ln \frac{hk_{\text{r}}}{k_{\text{B}}T} = \Delta S^{\ddagger} - \frac{\Delta H^{\ddagger}}{T} - R \ln \left\{ 1 + e^{\left(\frac{\Delta \Delta H^{\ddagger}}{T} - \Delta \Delta S^{\ddagger}\right)/R} \right\} \quad (2)$$

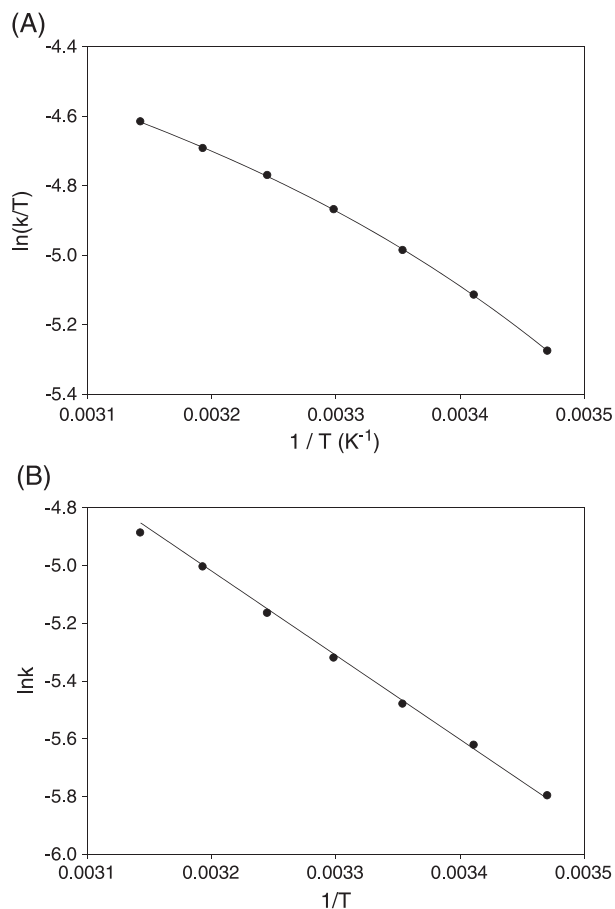


FIGURE 1 A, Eyring plot of $\ln k/T$ versus $1/T$ for the hydroxide hydrolysis of acetic anhydride at an ionic strength of 0.123M; B, Arrhenius plot of $\ln k$ versus $1/T$ for the hydrolysis of N,N-dimethylformamide at an ionic strength of 2.0M

where κ is the transmission coefficient; k_B is Boltzmann constant, and h is Planck constant.

Figure 1 below shows a typical Eyring plot.

The calculated values for activation energy, enthalpy, entropy, and free energy are provided in Table 1.

5 | PROTON INVENTORY FOR ACETIC ANHYDRIDE HYDROXIDE (BASE-CATALYZED) HYDROLYSIS

Data for $\frac{k_d}{k_h}$ vs mole fraction was applied to the proton inventory technique. A plot of $\frac{k_d}{k_h}$ vs mole fraction for acetic anhydride is shown in Figure 2.

TABLE 1 Activation parameters showing the difference in the isotope effects between acetic anhydride and DMF at 25°C

Parameter	Amide	Amide - D ₂ O	D _{kie}	Anhydride	Anhydride - D ₂ O	D _{kie}
E_a (kJ/mol)	56.2 (±0.4)	46.9(±0.4)	1.20 (±0.03)	40.8 (±17.9)	42.9 (±0.6)	**
ΔH^\ddagger (kJ/mol)	53.7(±0.7)	44.4 (±1.4)	1.21 (±0.03)	20.1 (±3.7)	38.2 (±3.4)	0.526 (±0.03)
ΔS^\ddagger (J/K*mol)	-51.6	-28.3(±4.6)	1.82 (±0.03)	-47.9 (±11.1)	-0.4 (±11.1)	**

**could not be determined.

The Gross-Butler equation was used to understand the mechanisms and propose the transition state structures for hydrolyses of acetic anhydride and DMF in hydroxide-catalyzed medium. The Gross Butler equation is given in Equation 3:

$$\frac{k_d}{k_h} = \frac{(1-x_d + \phi_i x_d)^{n_i}}{(1-x_d + \phi_j x_d)^{n_j}} \quad (3)$$

where ϕ and n in Equation 3 are the fractionation factor and the number of protons having a fractionation factor of ϕ . Table 2 shows results of nonlinear regression analyses of Equation 3 for the basic hydrolysis of acetic anhydride. Upon examining the values for $\phi = 0.498$ and 0.9292 for $n_1 = 1$ and $n_2 = 3$, respectively, $\phi = 0.498$ shows a significant change in the force field and implies a proton in-flight. The other 3 protons with ϕ values near unity show very little change in the force field.

6 | PROTON INVENTORY FOR DMF HYDROXIDE (BASE-CATALYZED) HYDROLYSIS

Unlike acetic anhydride, DMF shows an inverse kinetic isotope effect. The proton inventory data for hydrolysis of DMF is presented in Figure 3. The Gross-Butler equation was modified for the hydrolysis of DMF and as shown in Equation 4.

$$Y = \frac{(1-X + xa)(1-x + xb)(1-x + xc)}{(1-x + xd)(1-x + xe)} \quad (4)$$

The resulting plot is shown in Figure 3, and the inventory data is in Table 3.

The proton inventory analyses were performed using Equations 5 and 6, which indicate 6 and 10 protons, respectively.

$$Y = (1-x + xa)(1-x + xb)^2(1-x + xc)^3 \quad (5)$$

$$Y = \frac{(1-x + xa)(1-x + xb)^2(1-x + xc)^3}{(1-x + xd)(1-x + xe)^3} \quad (6)$$

The data are summarized in Tables 4 and 5.

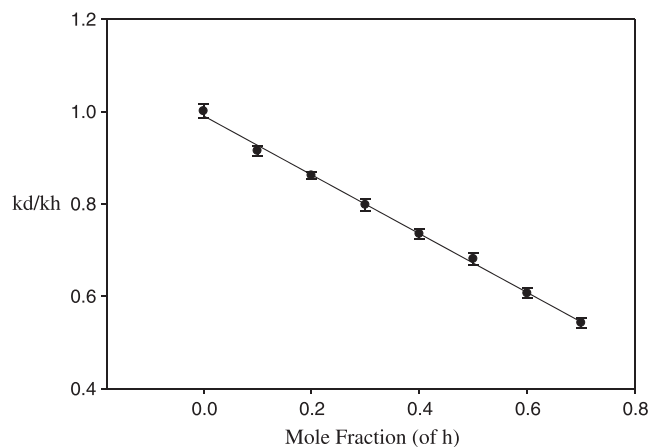


FIGURE 2 A typical plot of $\frac{k_d}{k_h}$ vs mole fraction (of h)

TABLE 2 Results of proton inventory analysis for the hydrolysis of acetic anhydride in 0.1M hydroxide solution at 25°C

Number of protonic sites	Regression coefficient	Values for ϕ
$n_1 = 1$	0.9971	0.5075
$n_2 = 1$		0.75
$n_1 = 1$	0.9980	0.4873
$n_2 = 2$		0.8918
$n_1 = 2$	0.9979	0.6110
$n_2 = 2$		1.0249
$n_1 = 1$	0.9980	0.498
$n_2 = 3$		0.9292

Since the suitable Gross-Butler equation to study the hydrolysis of DMF would be the Equation 4 (according to the R^2 coefficient), the proton inventory analysis of DMF had 10 protons in its transition state corresponding to 5 water molecules aiding the hydrolysis.

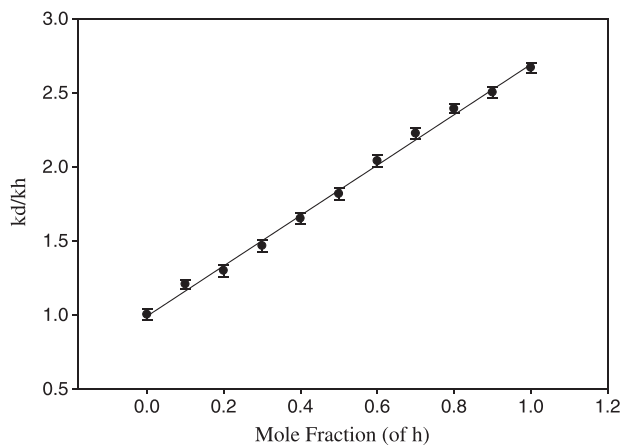


FIGURE 3 Gross-Butler plot for hydrolysis of N,N-dimethylformamide

TABLE 3 Proton inventory data for hydrolysis of N,N-dimethylformamide, which is best fit to Equation 6

$n_1 = 1$	$R^2 = 0.9991$	$a = 1.401$
$n_2 = 2$		$b = 1.33$
$n_3 = 3$		$c = 0.503$
$n_4 = 1$		$d = 0.598$
$n_5 = 3$		$e = 0.601$

TABLE 4 Proton inventory data corresponding to Equation 5

$n_1 = 1$	$R^2 = 0.9981$	$a = 1.756$
$n_2 = 2$		$b = 1.675$
$n_3 = 3$		$c = 0.817$

TABLE 5 Proton inventory data corresponding to Equation 6

$n_1 = 1$	$R^2 = 0.9971$	$a = 2.651$
$n_2 = 3$		$b = 1.021$
$n_3 = 3$		$c = 1.024$
$n_4 = 1$		$d = 1.038$
$n_5 = 3$		$e = 1.032$

7 | KINETIC ISOTOPE EFFECT

The kinetic isotope effects at various temperatures are presented in Table 6.

These values show decreasing normal $k_{i,e}$ values for acetic anhydride with increasing temperature. An inverse primary kinetic isotope effect is observed for DMF. A $k_{i,e}$ value decreases with increasing temperature for DMF. Table 7

TABLE 6 Temperature dependent $k_{i,e}$ values

Temp (°C)	k_h/k_d (anhydride)	k_h/k_d (amide)
15	2.652 (± 0.03)	0.314 (± 0.005)
20	2.812 (± 0.03)	0.430 (± 0.005)
25	2.795 (± 0.03)	0.391 (± 0.005)
30	3.037 (± 0.03)	0.358 (± 0.005)
35	2.714 (± 0.03)	0.475 (± 0.005)
40	2.645 (± 0.03)	0.551 (± 0.005)
45	2.425 (± 0.03)	0.512 (± 0.005)

TABLE 7 The rate constants of hydrolysis of acetic anhydride and DMF in solutions of varying alcohol mole fractions at 25°C and an ionic strength of 2.0M for DMF and 0.123M for acetic anhydride

Alcohol	k/s^{-1} (acetic anhydride)	k/s^{-1} (DMF)
No alcohol	0.00250 (± 0.00005)	0.00110 (± 0.00005)
Cyclohexanol (0 χ)	0.00260 (± 0.00005)	0.00110 (± 0.00005)
1-octanol (0 χ)	0.00280 (± 0.00005)	0.00110 (± 0.00005)

Abbreviation: DMF, N,N-dimethylformamide.

shows results of conducting the reactions in solutions of varying mole fractions of cyclohexanol and 1-octanol. There are no discernible solvent effects for DMF under these conditions within the statistical errors of the rate constants. However, for acetic anhydride, there is a slight discernable solvent effect. Making the solvent more nonpolar increases the rate of hydrolysis for acetic anhydride.

8 | SOLVENT EFFECTS

The effect of solvent on the rates of hydrolysis was studied in the presence of sodium chloride for both acetic anhydride and DMF. Sodium chloride decreased the rate of hydrolysis of acetic anhydride. Ionic strength had no effect on the rate of DMF hydrolysis. At 25°C, using the limiting law of the Debye Huckel equation, the rate of hydrolysis of acetic anhydride at 5 concentrations of sodium chloride (0M, 1M, 2M, and 3M) were plotted against the square root of the ionic strength of sodium chloride. This plot is shown in Figure 4.

The transition state structure involved in the base-catalyzed hydrolysis of acetic anhydride has 2 water molecules corresponding to 4 protons with 1 hydrogen being in flight (Figure 2). The rate constant obtained for acetic anhydride hydrolysis at 30°C and 0.123M NaOH was 0.0041 s^{-1} . Of this rate, $k_{\text{simple}} = 0.00312 \text{ s}^{-1}$. Therefore, $k_{\text{OH}} = (k - k_{\text{simple}}) / [\text{OH}]/[\text{H}_2\text{O}] = 0.539 \text{ s}^{-1}$. Thus, 76% of hydrolysis is due to simple hydrolysis (at 0.123M hydroxide concentration). This was determined using the plot from the salt effect study and fitting to a polynomial (quadratic) equation. Once, the equation was obtained, the rate for simple hydrolysis at 25°C at 0.123 M ionic strength was found. Therefore, k_{OH} in H_2O and D_2O were determined.

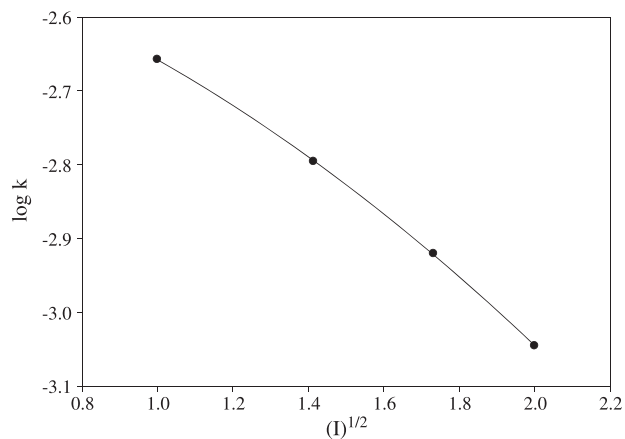


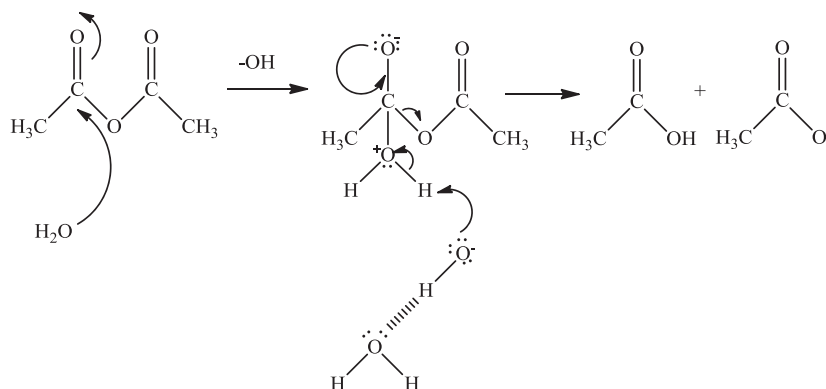
FIGURE 4 Ionic strength dependence for the hydrolysis of acetic anhydride in presence of sodium chloride at 25°C and 0M NaOH

9 | BASE-CATALYZED ACETIC ANHYDRIDE HYDROLYSIS

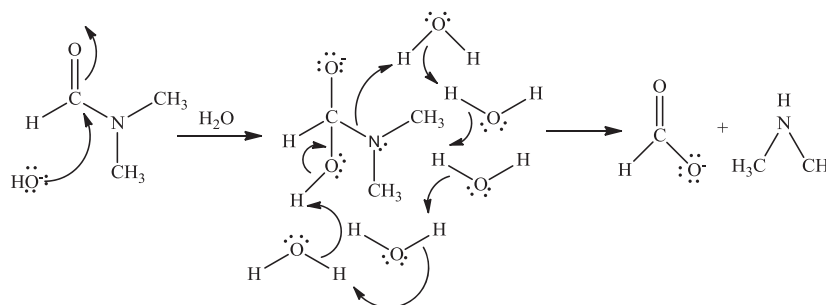
For the mechanism (for base-catalyzed acetic anhydride hydrolysis) corresponding to experimental data fitted to the Gross-Butler equation, the conclusion was made (in the current study) that hydroxide, solvated by a single water molecule, assists in the attack as shown in Scheme 2 and not the nucleophile. Current data shows that 1 proton has a fractionation factor value of 0.49 that corresponds to the proton in flight, and the 3 protons have fractionation factor values of 0.929, which do not undergo any significant change in the force field. If hydroxide was the nucleophile being assisted by 2 water molecules, then there would possibly be 2 protons in flight with fractionation factors around 0.5 and 3 protons with fractionation factors around 0.9. This corresponds to an incorrect number of protons. In light of ΔH^{\ddagger} dkie equals a large inverse isotope effect, 0.526, which implies bonds are stronger in the transition state than in the reactants state. In addition, the curvature of the Eyring plot in Figure 1 suggests that the acetic anhydride hydrolysis is a 2-step process as illustrated in Scheme 2. Again, curved arrows represent the flow of electrons. In addition, 1 particular arrow in the following scheme is showing that the electrons are flowing from and O—H sigma bond to an H|||O hydrogen bond. By doing so, this illustration signifies that an O—H sigma bond is breaking and a sigma bond is forming at the site of the H|||O hydrogen bond.

10 | BASE-CATALYZED DMF HYDROLYSIS

Based on the kinetic solvent effect data from Scheme 3, it was assumed that transition state of DMF has to be neutral charge on the molecule with a negative 1 on the hydroxide (which is in agreement with Cox^[38]). Since the rates of hydrolysis do not change with added concentrations of salt, this may mean that there is no major redistribution of charge between the reactant and transition structures (as shown in the current study). Since hydroxide is the nucleophile, then by attacking the carbonyl, carbon creates a negative charge on the carbonyl oxygen. However, the amide nitrogen gets protonated and assumes a plus 1 charge (which counters the negative 1 of oxygen). Overall, the charge is neutral on the transition state of DMF. The point of difference between acetic anhydride and DMF may be how the charge redistributes in the respective transition states. One possibility is a later transition state for acetic anhydride hydrolysis. The transition state for DMF would be early. In the transition state, the mass of the hydrogen or that of the deuterium will affect the vibration in the same way as that in the reactant. The transition state structure of DMF has 10 protons in the transition



SCHEME 2 Mechanism for the hydrolysis of acetic anhydride



SCHEME 3 Mechanism involved in the hydrolysis of N,N-dimethylformamide

state where 7 protons are in flight (consistent with Šlebocka-Tilk conclusion that there are 5 water molecules in the transition state). In light of the activation energy, the d_{kic} is insignificant ($=1.20$). However, for ΔS^\ddagger , there is a d_{kie} ($=1.82$) that implies that the bonds are stronger in the reactants state than in the transition state. There are 2 water molecules assisting the hydroxide, 1 water molecule is involved in protonating the amide nitrogen, and 2 water molecules are involved in protonating the carbonyl oxygen (Scheme 3). This is consistent with the proton inventory fit and analyses that includes 3 protons of 1 type are in flight, 3 other protons of another type are in flight, and 1 proton of a third type is in flight (the reaction for DMF hydrolysis at pH 7.0 at 25°C was attempted. However, under these conditions, no reaction took place. Only under strong hydroxide base catalyzed hydrolysis does a reaction occur).

11 | CONCLUSION

Table 1 indicates that the free energy barrier for the hydrolysis of amide in nondeuterated media is higher than the barrier in deuterated media. Hence, reactant, DMF, has to cross the higher barrier to reach the transition state in nondeuterated media making the reaction slower. In the case of acetic anhydride, the free energy barrier is smaller for hydrolysis in nondeuterated media. Hence, the reactant has to cross a higher barrier in deuterated media to reach the transition state. Hence, the rate of hydrolysis of acetic anhydride is

higher in nondeuterated media than in deuterated media. Studies on the rates of hydrolysis of acetic anhydride and DMF in the solutions of decreasing polarity show that the transition state of acetic anhydride is less polar than the reactants. The polarity of the activated complex of DMF is equal to the reactants due to numerous water molecules in the transition state. Experiments on kinetic salt effect showed that the rate of hydrolysis of DMF did not change with the added concentrations of inorganic or organic salt suggesting sodium chloride or sodium acetate did not affect the charge on the reactants. In the case of acetic anhydride, sodium chloride had a negative effect on the rate of hydrolysis and the charge of ions involved in the formation of activated complex is $-0.378 e$ (which has never been shown before this current study) is tabulated from the following equation

$$\text{Log } K_{TS} = \text{log}K_O + 2AZ_AZ_B I^{1/2}$$

where Z is the charge of the cation and anion from the salt and K_O is the rate without salt present. The reactants have a charge of -1 for hydroxide, and 0 for the anhydride. This charge is distributed more in the transition structure of acetic anhydride hydrolysis but is still -1 due to the stoichiometry.

The assumption was made that an increase in the concentration of sodium chloride causes an increase in the charge on the formation of activated complex.^[39] Thus, since the reaction decreases with increasing solvent polarity, then it is likely that the transition structure is more nonpolar than the

reactants. This information will become most crucial in studies such of the role of water in enzymatic protein hydrolysis.^[40] To understand the role of water in the study of whey protein isolate, at 30% (w/v) whey protein isolate, the amount of water becomes limited. Therefore, a small decrease in observed water activity correlates to a large increase in bound water. This article provides a useful starting point in understanding the structure of water in the transition-state of enzyme-catalyzed hydrolysis of such systems.

REFERENCES

- [1] K. J. P. Orton, M. J. J. Jones, *Am. Chem. Soc.* **1912**, *101*, 1708.
- [2] F. A. Cleland, R. H. Wilhelm, *AIChE J.* **1956**, *2*, 489.
- [3] V. Gold, *Trans. Far. Soc.* **1948**, *44*, 506.
- [4] T. L. J. Smith, *Phys. Chem.* **1955**, *59*, 385.
- [5] H. J. Janssen, C. H. Haydel, L. H. Greathouse, *Ind. Eng. Chem.* **1957**, *49*, 197.
- [6] D. Glasser, D. F. Williams, *Ind. Eng. Chem. Fund.* **1971**, *10*, 516.
- [7] A. C. D. Rivett, N. V. J. Sidgwick, *Am. Chem. Soc.* **1910**, *97*, 732.
- [8] A. K. J. Kralj, *Ind. Eng. Chem.* **2007**, *13*, 631.
- [9] W. C. Bell, K. S. Booksh, M. L. Myrick, *Anal. Chem.* **1998**, *70*, 332.
- [10] S. Haji, C. Erkey, *Chem. Eng. Ed.* **2005**, *39*, 56.
- [11] S. P. Asprey, B. W. Wojciechowski, N. M. Rice, A. Dorcas, *Chem. Eng. Sci.* **1996**, *51*, 4681.
- [12] A. Zogg, U. Fischer, K. Hungerbuhler, *Chemom. Int. Lab. Sys.* **2004**, *71*, 165.
- [13] G. Puxty, M. Maeder, R. R. Rhinehardt, S. Alam, S. Moore, P. J. J. Gemperline, *Chem. Commun.* **2005**, *19*, 329.
- [14] F. L. J. Wiseman, *Phys. Org. Chem.* **2012**, *25*, 1105.
- [15] M. C. Cook, A. Bliu, J. P. Kunkel, *Vaccine* **2012**, *30*, 3702.
- [16] J. Lu, H. Yang, J. Hao, C. Wu, L. Liu, N. Xu, R. J. Linhardt, Z. Zhang, *Carb. Poly.* **2015**, *122*, 180.
- [17] M. A. Rahman, Z. Iqbal, M. A. Mirza, A. Hussain, *Pharm. Meth.* **2012**, *3*, 62.
- [18] H. Li, Q. Qing, R. Kumar, C. J. Wyman, *Ind. Microb. & Biotech.* **2013**, *40*, 551.
- [19] D. Ellington, T. Pritchard, P. Foy, K. King, B. Mitchell, J. Austad, D. Winters, D. J. Sullivan, *AOAC Int.* **2012**, *95*, 1469.
- [20] A. J. Scheidig, C. Burmester, R. S. Goody, *Structure* **1999**, *7*, 1311.
- [21] N. Okimoto, T. Tsukui, M. Hata, T. Hoshino, M. Tsuda, *J. Am. Chem. Soc.* **1999**, *121*, 7349.
- [22] N. Okimoto, T. Tsukui, *J. Am. Chem. Soc.* **2000**, *122*, 5613.
- [23] R. A. Khalil, A. H. Jalil, A. Y. J. Abd-Alrazzak, *Iran. Chem. Soc.* **2009**, 345.
- [24] O. Moukha-Chafiq, R. C. Reynolds, *Nucleos. Nucleot. & NA* **2014**, *33*, 709.
- [25] E. Kilinc, B. Gumgum, C. Hamamci, F. Aydin, *Anal. Chem.* **2009**, *64*, 714.
- [26] G. Orsomando, G. G. Bozzo, R. D. de la Garza, G. J. Basset, E. P. Quinlivan, V. Naponelli, F. Rebeille, S. Ravel, J. F. Gregory, A. D. Hanson, J. Plant, *Cell & Mole. Biol.* **2006**, *46*, 426.
- [27] H. Šlebocka-Tilk, A. A. Neverov, R. S. J. Brown, *Am. Chem. Soc.* **2003**, *125*, 1851.
- [28] J. F. Marlier, N. C. Dopke, K. R. Johnstone, T. J. Wirdzig, *J. Am. Chem. Soc.* **1999**, *121*, 4356.
- [29] Y. Xiong, C. J. Zhan, *Phys. Chem. A* **2006**, *110*, 12644.
- [30] K. R. Lynn, P. E. J. Yankwich, *Phys. Chem.* **1960**, *64*, 1719.
- [31] J. I. Mujika, E. Formoso, J. M. Mercero, X. J. Lopez, *Phys. Chem. B* **2006**, *30*, 15000.
- [32] P. Linda, A. Stener, A. Cipiciani, G. J. Savelli, *Hetero. Chem.* **1983**, *20*, 247.
- [33] J. F. Mata-Segreda, *Isotopes in Environ. and Health St.* **2007**, *43*, 17.
- [34] K. J. Laidler, M. C. J. King, *Phys. Chem.* **1983**, *87*, 2657.
- [35] C. A. Bunton, N. A. Fuller, S. G. Perry, I. H. J. Pitman, *Am. Chem. Soc.* **1962**, *867*, 4478.
- [36] F. A. Carroll, *In Perspective on Structure and Mechanism in Organic Chemistry*, 2nd ed., John Wiley & Sons, Hoboken, NJ **2010**.
- [37] F. L. Wiseman, W. C. Cooper, B. Robinson, *Intrntnl. J. Avd. Res. Chem. Sci.* **2015**, *2*, 1.
- [38] R. A. Cox, *Can. J. Chem.* **2005**, *83*, 1391.
- [39] P. W. Atkins, J. de Paula, *Physical Chemistry*, 9th ed., Oxford University Press, Oxford, UK **2010**.
- [40] C. I. Butre, P. A. Wierenga, H. Gruppen, *Process Biochem.* **2014**, *49*, 1903.

How to cite this article: Cooper WC, Chilukoorie A, Polam S, Scott D, Wiseman F. A comparative study on the hydrolysis of acetic anhydride and N,N-dimethylformamide: Kinetic isotope effect, transition-state structure, polarity, and solvent effect. *J Phys Org Chem.* 2017;e3701. <https://doi.org/10.1002/poc.3701>